

A GENUINELY MULTIDISCIPLINARY JOURNAL

CHEMPLUSCHEM

CENTERING ON CHEMISTRY

Accepted Article

Title: Carbazole-Terpyridine Donor-Acceptor Dyads with Rigid π -Conjugated Bridges

Authors: Nicola Armaroli, Elia Matteucci, Andrea Baschieri, Letizia Sambri, Filippo Monti, Eleonora Pavoni, and Elisa Bandini

This manuscript has been accepted after peer review and appears as an Accepted Article online prior to editing, proofing, and formal publication of the final Version of Record (VoR). This work is currently citable by using the Digital Object Identifier (DOI) given below. The VoR will be published online in Early View as soon as possible and may be different to this Accepted Article as a result of editing. Readers should obtain the VoR from the journal website shown below when it is published to ensure accuracy of information. The authors are responsible for the content of this Accepted Article.

To be cited as: *ChemPlusChem* 10.1002/cplu.201900213

Link to VoR: <http://dx.doi.org/10.1002/cplu.201900213>

WILEY-VCH

www.chempluschem.org

A Journal of



Carbazole-Terpyridine Donor-Acceptor Dyads with Rigid π -Conjugated Bridges

Elia Matteucci,^[a] Andrea Baschieri,^{*[b]} Letizia Sambri,^{*[a]} Filippo Monti,^{*[c]} Eleonora Pavoni,^[c] Elisa Bandini,^[c] and Nicola Armaroli^{*[c]}

Abstract: A series of molecules (1-7) in which 9*H*-carbazole (electron donor, D) and 2,2':6',2''-terpyridine (electron acceptor, A) are connected through rigid π -conjugated bridges (D- π -A systems) have been synthesized and their photophysical properties examined in detail, with the support of DFT calculations. The bridges are made of different sequences of ethynylene, phenylene and anthracene groups. The synthetic strategies involve condensation of 2-acetylpyridine with the aromatic aldehyde moiety on different functionalized π -conjugated bridges and couplings with carbazole derivatives. The system incorporating anthracene in the bridge (7) shows the typical absorption and emission fingerprints of this π -extended system. 1-6 have HOMOs and LUMOs centered, respectively, over the carbazole and the bridge and exhibit solvatochromic charge-transfer (CT) luminescence with high photoluminescence yield up to 70%, except when an ethynylene unit is directly attached to the carbazole ring (2,6), due to a trans-bent non emissive π - σ^* excited state.

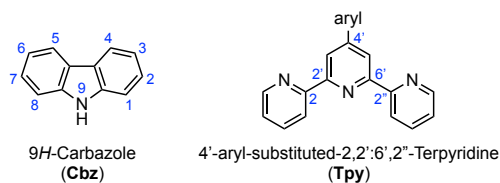
Introduction

Organic conjugated systems exhibit wide interest as functional materials in several applications.^[1-7] They are generally easy to prepare at low cost and their electronic and optical properties can be predicted to a good extent, therefore displaying remarkable advantages over inorganic materials. Accordingly, they are extensively used as active layers in a variety of organic devices, such as light-emitting diodes (OLEDs),^[8] field-effect transistors (OFETs),^[9] photovoltaic cells (OPVC),^[5,10,11] dye-sensitized solar cells (DSSC)^[12] sensors^[13,14] as well as in bioimaging applications.^[15,16]

Among many options for the design of organic π -conjugated molecules, the combination of an electron donor (D) and a related

acceptor (A) is particularly interesting, as it affords "push-pull" systems, which are well suited for organic electronics, semiconductors and photovoltaics.^[17] The A/D subunits can be covalently connected through different rigid and conjugated systems, so as to prepare D- π -A architectures^[18-23] which may show a characteristic photophysical behaviour, in particular charge-transfer absorption (and possibly emission) bands, typically red-shifted compared to spectral features arising from local excited states centered on the individual subunits.^[24]

Electron-rich moieties containing fused aromatic rings can exhibit high carrier mobilities, enhanced fluorescence and reduced band gaps. Among them, 9*H*-carbazole (**Cbz**, Scheme 1) is a popular molecular platform made of a fused tricyclic structure with good planarity and high stability, thanks to its fully aromatic configuration.^[25-27] The presence of a nitrogen atom in the 9 position enables easy coupling with other functional groups, without altering the electronic and photophysical properties of the molecule. Moreover, 1-C to 8-C positions can be easily functionalized with suitable groups, opening the route to the synthesis of many carbazole-based derivatives.^[28,29]



Scheme 1. Chemical structure and numbering of the donor (**Cbz**) and acceptor (**Tpy**) units used for the synthesis of the investigated dyads.

9*H*-Carbazole and its derivatives have been extensively used as electron donating (D) units in π -conjugated small molecules and polymers.^[30,31] On the other hand, 2,2':6',2''-terpyridine and its derivatives are readily accessible molecules widely used in organic and supramolecular chemistry, due to their electron accepting (A) character and, most remarkably, to the ability of serving as tridentate ligands,^[32] also largely used in photoactive polynuclear metal complexes.^[33-36] Moreover, they can be used as proton responsive units in multicomponent arrays.^[37]

Previous studies have shown that 4'-aryl-substituted 2,2':6',2''-terpyridine derivatives (**Tpy**, Scheme 1) exhibit excellent luminescence properties.^[38,39] These compounds can be synthesized in one-pot under environmentally benign conditions, via condensation of 2-acetylpyridine with different aromatic aldehydes.^[40,41] The 1,5-diones intermediates thus obtained are then cyclized, without prior isolation, by adding concentrated aqueous ammonia and affording the desired substituted terpyridines.

[a] Dr. E. Matteucci, Prof. L. Sambri
Dipartimento di Chimica Industriale "Toso Montanari"
Università di Bologna
Viale Risorgimento 4, 40136 Bologna, Italy
E-mail: letizia.sambri@unibo.it

[b] Dr. A. Baschieri
Dipartimento di Chimica "Giacomo Ciamician"
Università di Bologna
Via San Giacomo 11, 40126 Bologna, Italy
E-mail: andrea.baschieri2@unibo.it

[c] Dr. F. Monti, Dr. E. Pavoni, Dr. E. Bandini, Dr. N. Armaroli
Istituto per la Sintesi Organica e la Fotoreattività
Consiglio Nazionale delle Ricerche
Via Piero Gobetti 101, 40129 Bologna, Italy
E-mail: filippo.monti@isof.cnr.it, nicola.armaroli@isof.cnr.it

Supporting information for this article is given via a link at the end of the document.

FULL PAPER

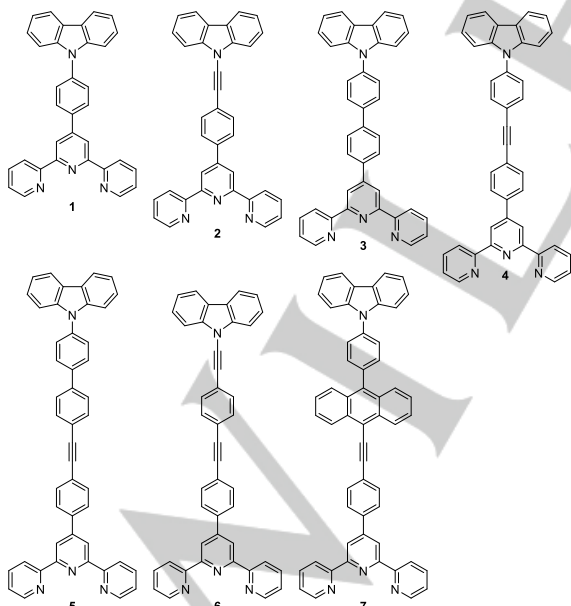
A vast number of derivatives containing carbazole or terpyridine units can be found in the literature, but relatively few reports on compounds carrying both units separated by a π -conjugated system.^[42-47] Therefore, there is room for developing new carbazole-terpyridine derivatives with enhanced optoelectronic features, also to widen our knowledge on the relationship between the structure and the electronic properties.^[48] Our earlier work carried out on this type of molecules showed that the absorption and emission properties of carbazole-terpyridine dyads can be finely tuned by changing the spacers between the two terminal subunits.^[49]

With the aim of expanding the availability and scope of this versatile class of D- π -A compounds, herein we report a new series of carbazole-terpyridine systems where the two terminal units are connected through aromatic and triple bonds spacers. In this way, the conjugation degree is tuned in an effort to obtain stable architectures with high photoluminescence quantum yields (PLQYs). In perspective, the presence of the free terpyridyl group makes these systems suitable for chelation of transition metals, opening the route to new photoactive coordination compounds.

Results and Discussion

Synthesis of the dyads

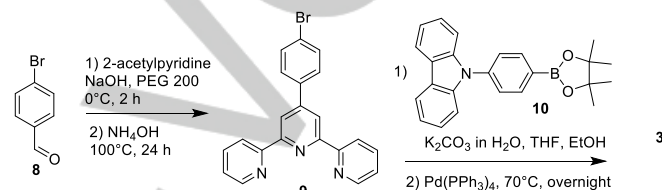
Expanding our previous approach to the preparation of Cbz-Tpy dyads such as **1** and **2** (Scheme 2), we have designed and synthesized five new carbazole-terpyridine derivatives (**3-7**), in which the π -conjugated bridge between the donor and acceptor units is progressively elongated with acetylene, phenylene and even anthracene units.



Scheme 2. Chemical structure of compounds 1-7.

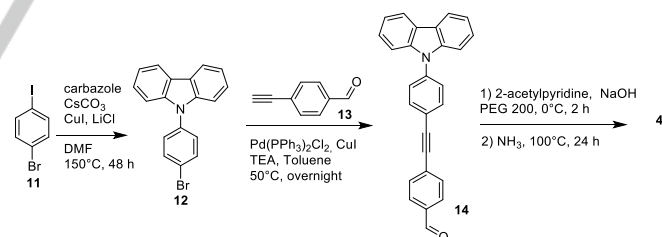
The synthetic approach is based on the preliminary preparation of the properly functionalized π -conjugated bridge, on which the carbazole unit is grafted and the terpyridine moiety is formed through a one-pot condensation reaction.^[40,41] The detailed synthetic procedures affording the new compounds **3-7** are described herein.

Dyad **3** is obtained in two steps (Scheme 3). First the condensation of the commercially available *p*-bromobenzaldehyde with 2-acetylpyridine in the presence of NaOH and ammonia leads to the terpyridine intermediate **9** in 73% yield. The latter is then reacted with 9*H*-carbazole-9-(4-phenyl) boronic acid pinacol ester **10** through a Suzuki coupling, giving the target product **3** in 25% yields.



Scheme 3. Synthesis of dyad 3.

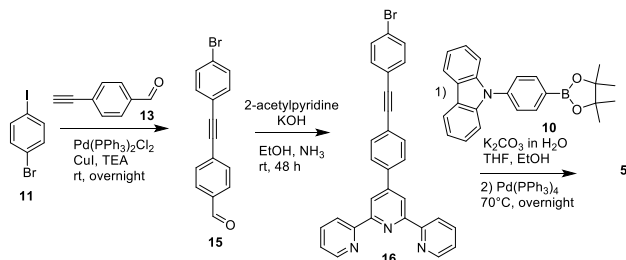
Compound **4** is prepared through a selective Ullman-type condensation of *p*-iodo-bromobenzene **11** with 9*H*-carbazole promoted by Cu(I),^[50] which gives **12** in 71% yield (Scheme 4). This intermediate is then reacted with *p*-ethynyl benzaldehyde **13** in a palladium-catalysed Sonogashira coupling, affording the aldehyde **14** in 22% yield, which is finally condensed with 2-acetylpyridine to form the terpyridine moiety and give compound **4** in 35% yield.



Scheme 4. Synthesis of dyad 4.

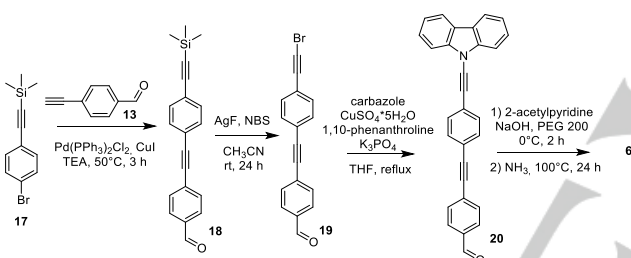
Similarly to **4**, the first step of the synthesis of **5** started from *p*-iodo-bromobenzene **11** with *p*-ethynyl benzaldehyde through a Sonogashira coupling to give the intermediate **15** equipped with both aldehyde and bromine functionalities in 94% yield (Scheme 5). Eventually, the terpyridine moiety is assembled by reaction of **15** with 2-acetylpyridine in the presence of KOH and ammonia in 15% yield to obtain **16**. The target product **5** is obtained by Suzuki coupling of **16** with 9*H*-carbazole-9-(4-phenyl) boronic acid pinacol ester **10** in 30% yields.

FULL PAPER



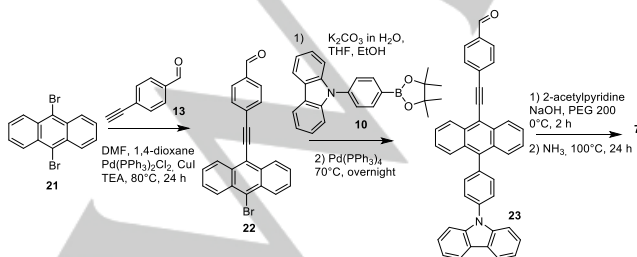
Scheme 5. Synthesis of dyad 5.

In Scheme 6 is depicted the synthesis of **6**. The TMS-protected *p*-ethynyl-bromobenzene **17** undergoes a palladium-catalysed Sonogashira coupling with *p*-ethynylbenzaldehyde **13**, giving the intermediate **18** in 44% yield, which reacts with *N*-bromosuccinimide and AgF leading to the bromo-derivative **19** in 78% yield. The latter reacts with 9*H*-carbazole in an Ullmann-type copper(II) catalysed coupling, giving the carbazole derivative **20** (47% yield), which affords the desired product **6** upon condensation with 2-acetylpyridine and ammonia in 15% yield.



Scheme 6. Synthesis of dyad 6.

Dyad **7** includes an anthracene moiety as spacer, in order to increase the π -delocalization with respect to the analogue **5**. The synthesis (Scheme 7) starts from 9,10-dibromoanthracene **21**, which undergoes a palladium-catalysed Sonogashira coupling with *p*-ethynylbenzaldehyde, giving the mono-substituted intermediate **22** (35% yield). The latter is then reacted with 9*H*-carbazole-9-(4-phenyl) boronic acid pinacol ester **10** through a Suzuki coupling to afford the carbazole intermediate **23** in 38% yield. The latter undergoes final condensation of the terminal aldehyde with 2-acetylpyridine, giving **7** in 15% yield.



Scheme 7. Synthesis of dyad 7.

With the exception of the condensation step giving the terpyridine, which occurs with moderate yields, the other synthetic steps are generally efficient. However, the purification of the final products turned out to be difficult. Separation of impurities (primarily terpyridine derivatives with almost the same polarity) was difficult and common purification procedures such as column chromatography generally failed. Alternatively, we opted for techniques that take advantage of the low solubility of the final compounds in polar solvent (see Experimental Part). Due to these problems, the overall yields of the final derivatives were sometimes low, but the high purity achieved allowed extensive structural and photophysical characterizations.

Ground-state theoretical calculations

All the investigated molecules display an ideal C_2 symmetry in their optimized ground-state geometries. This is because these carbazole-terpyridine dyads have been designed with rigid linear bridges of different lengths, so that the donor (carbazole) and the acceptor (terpyridine) moieties are separated by π -conjugated spacers of well-defined lengths, but always in the direction of the main molecular axis. In Table 1 are listed key calculated structural geometric parameters of the investigated dyads, including the calculated distances between the centroids of the carbazole-donor and terpyridine-acceptor moieties (d_{DA}).

Table 1. Structural geometric parameters of the dyads, calculated at the M06-2X/6-31+G(d) level of theory in toluene (using PCM).

S ₀ optimized geometry				S ₀ → S ₁ excitation ^[a]			
Conf. ^[b]	d _{DA} [Å]	α _{DA} ^[c] [deg.]	Energy [eV]	Oscillator strength	D _{CT} [Å]	D _{CT} /d _{DA}	
1	2	10.71	18.8	4.20	0.744	5.11	0.48
		10.71	89.0	4.20	0.700	5.22	0.49
2	1	13.28	29.0	3.97	1.67	4.67	0.35
		15.02	21.9	4.22	1.38	4.88	0.32
3	4	15.02	50.1	4.22	1.34	5.15	0.34
		15.02	52.3	4.21	1.37	4.95	0.33
		15.02	58.7	4.22	1.33	5.14	0.34
		17.60	23.5	3.84	1.99	4.28	0.24
4	2	17.60	88.6	3.84	1.99	4.27	0.24
		21.91	22.0	3.85	2.79	2.71	0.12
5	4	21.91	49.1	3.85	2.76	2.78	0.13
		21.91	53.4	3.85	2.79	2.72	0.12
		21.91	56.7	3.85	2.76	2.79	0.13
		21.17	30.5	3.64	2.74	3.87	0.18
6	1	21.93	12.8	3.01	1.07	0.35	0.02
		21.93	17.5	3.01	1.07	0.35	0.02
		21.93	62.2	3.02	1.06	0.35	0.02
		21.93	87.2	3.01	1.07	0.27	0.01

[a] Lowest-energy transition computed at the ground-state minimum-energy geometry using TD-DFT methods and the PCM linear response formalism. [b] Number of unique conformational minima. [c] Dihedral angle between the plane of the carbazole and of the terpyridine moiety.

FULL PAPER

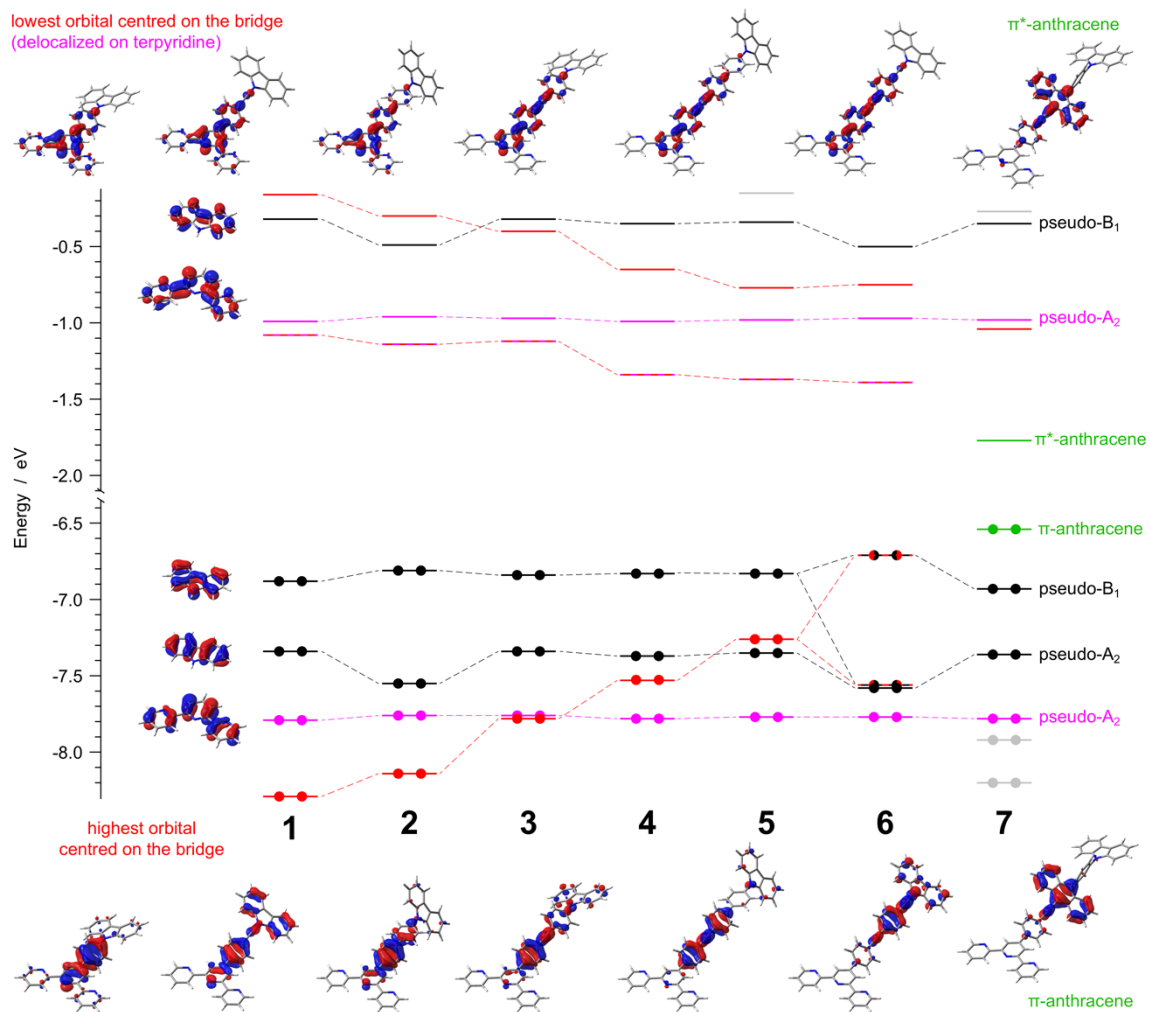


Figure 1. Frontier molecular orbitals of 1–7, calculated in toluene at the M06-2X/6-31+G(d) level of theory.

The adopted spacers belong to the class of biphenyl and/or tolane (*i.e.*, diphenylacetylene) *para*-derivatives. Accordingly, the corresponding dyads can adopt a large number of virtually isoenergetic conformations, which are generated by the reciprocal orientations of the optimal dihedral angles between the different moieties of the dyads (Tables S1–S7). While the tolane unit is known to be planar,^[51,52] the biphenyl one displays torsional angles of about 40°, depending on the environment.^[53,54] As a consequence, the dihedral angle between the plane of the carbazole and of the terpyridine moiety (*i.e.*, α_{DA} in Table 1) can vary substantially within the different minima of a specific dyad, ranging from nearly coplanar to almost perpendicular conformations (as in the simplest case of 1, see Table 1, Table S1 and Figure S1). However, it is worth noting that such conformers are in fast equilibration since rotations are virtually free at room temperature (Figure S2 and S3), especially when they occur around the ethynyl linker.^[55] The only notable exception is when the carbazole moiety is linked directly to a phenyl unit; in this case, a rather large barrier (*i.e.*, 63.5 kJ/mol)

prevents the carbazole to easily swap above or below the plane of the phenyl ring (as in the case of 1, see Figure S2, bottom).

In Figure 1 are reported the energy diagrams and the frontier molecular orbitals of all the dyads. As we previously reported for 1 and 2,^[49] the HOMO is predominantly centered on the carbazole moiety in all cases, with the notable exception of 7 which is equipped with an anthracene unit, providing a π orbital well above that of carbazole. As a consequence, the HOMO energy is almost constant in dyads 1–6 (*i.e.*, approx. -6.8 eV), while it is considerably higher for 7 (*i.e.*, -6.54 eV, Figure 1). On the other hand, the LUMO is mainly delocalized over the bridge and the central pyridine ring of the terpyridine acceptor. Also in this case, dyad 7 is an exception since its LUMO is centered only on the ethynyl-anthracene moiety of the bridge and the terpyridine π* orbitals start to play a role only in LUMO+1 and LUMO+2. Due to the extended delocalization of the LUMO over the molecular bridge, its energy changes much more markedly along the series; generally, the longer the bridge, the higher the delocalization, the lower the LUMO energy.

FULL PAPER

Since the orbitals are rather localized on a specific part of the dyads (*i.e.*, the carbazole-donor, the terpyridine-acceptor or the bridge), virtually no differences were observed in the energy and topology of the frontier molecular orbitals within a set of analogous conformers, regardless of the α_{DA} dihedral angle between the carbazole and terpyridine moieties, as representatively shown in Figure S4 for dyad **1**. Moreover, the ground-state properties are virtually not affected by the polarity of the solvent; in fact, both the optimized geometries and the energy and topology of molecular orbitals of all the dyads are almost identical, if calculated in toluene or in dimethylformamide (as representatively shown in Figure S5 for dyad **2**). Only a stabilization of around 0.1 eV is observed for all the frontier molecular orbitals in the more polar solvent.

Absorption properties

In Figure 2 are reported the absorption spectra of **1–7** in two solvents of different polarity, namely toluene and dimethylformamide (DMF). The selection of these two solvents allows to investigate the photophysical properties of all the donor-acceptor dyads in media having different dielectric constant, in which all the samples are completely soluble (*i.e.*, no aggregation phenomena) and where there is no risk of protonating the terpyridine unit (*i.e.*, protic solvents and/or solvents with potential acid impurities were not considered).

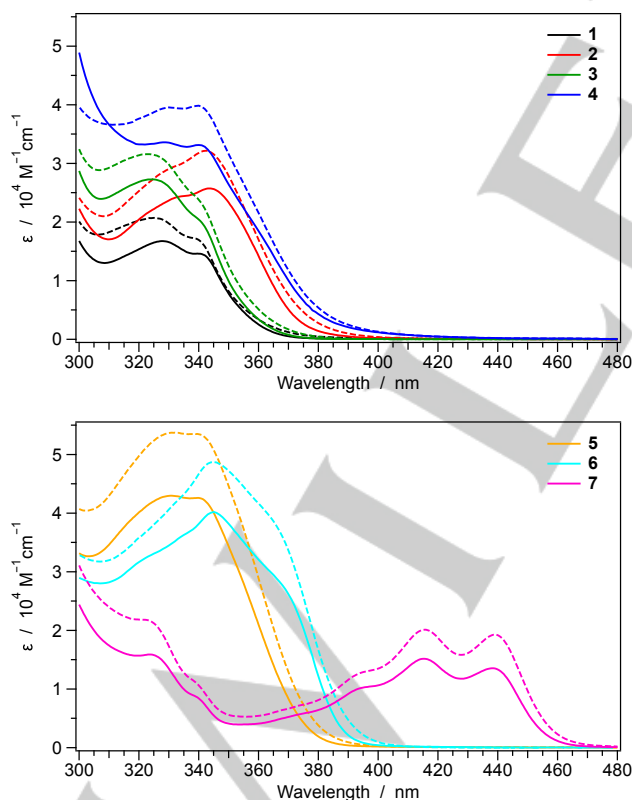


Figure 2. Absorption spectra of **1–7** in toluene (full lines) and dimethylformamide (dashed lines) at 298 K.

All of the species exhibit absorption features above 340 nm, unlike the individual moieties **Cbz** and 4'-*p*-tolyl-2,2':6',2''-terpyridine (**Ttpy**) (Figure S6). This may be tentatively attributed to low-energy carbazole \rightarrow terpyridine charge-transfer (CT) transitions.^[49] However, the absorption profiles of all dyads do not display a remarkable solvatochromism when spectra in toluene and dimethylformamide are compared (Figure 2).

Dyad **1** can be considered as the simplest donor-acceptor system of the series, since the carbazole donor is directly linked to the 4'-phenyl-terpyridine acceptor. In this archetypal array, the lowest-energy CT band corresponding to the $S_0 \rightarrow S_1$ electronic transition displays a maximum at approx. 325 nm (*i.e.*, 3.82 eV) both in toluene and dimethylformamide.

The addition of an ethynyl spacer, as in dyad **2**, causes a red shift of the lowest-energy absorption band of about 0.15 eV (*i.e.*, from 325 to 345 nm, approximately).

On the contrary, the absorption spectra of **1** and **3** are almost superimposable, suggesting that the insertion of one phenyl ring does not significantly affect the electronic properties of the corresponding dyad.

However, if an ethynyl spacer is added between the two phenyl moieties of **3** (*i.e.*, dyad **4**), a red shift of the $S_0 \rightarrow S_1$ electronic transition is again observed and the absorption profile of **4** turns out to be comparable to that of **2**, despite a different vibronic progression, a slightly red-shifted onset of the absorption band and higher molar absorption coefficients.

Notably, the absorption spectra of **4** and **5** are very similar, confirming that the addition of a phenyl ring on the carbazole side has negligible influence on both the energy and the profile of the lowest-energy absorption band of these dyads.

On the other hand, the replacement of the phenyl ring directly attached to the carbazole side with an ethynyl unit (**5** vs. **6**) is able to induce a red-shift of around 0.15 eV, as also observed when passing from **3** to **2**. Accordingly, dyad **6** displays the most red-shifted CT band of the whole series.

Differently from all the other dyads, the absorption spectrum of **7** extends well beyond 400 nm, due to the $\pi-\pi^*$ transition centered on the 9,10-disubstituted anthracene moiety of its bridge.^[56] As a consequence, this lowest-energy transition is vibronically structured and display no solvatochromism. This scenario is well predicted by TD-DFT calculations which estimate this excitation to occur at (3.02 ± 0.01) eV, regardless the polarity of the solvent (see below). On the other hand, for **7**, the first CT transition is calculated at (4.08 ± 0.01) eV above S_0 (*i.e.*, $S_0 \rightarrow S_3$ excitation in Table S14).

TD-DFT vertical excitations and analysis of the CT bands

In Table S8–S14 are reported the lowest singlet vertical excitations calculated by the TD-DFT approach, both in toluene and dimethylformamide. Due to the very high multiconfigurational character of these transitions, in order to get a compact orbital representation for the electronic transition density matrix, natural transition orbitals (NTOs) are used.^[57] The effect of the solvent polarity on the computed transitions is negligible, as also observed in the experimental absorption spectra (Figure 2). The

FULL PAPER

results obtained by the adopted M06-2X level of theory were also successfully compared to the ones calculated by the CAM-B3LYP^[58] and ω B97XD^[59] functionals, which are known to properly evaluate charge-transfer excitation energies^[60] and do not underestimate the energy of the transitions toward planar quinoid-like states in biphenyl.^[54]

In general, for dyads **1–6**, the first electronic transition always displays a strong CT character with high oscillator strength, the $S_0 \rightarrow S_2$ excitation is localized on the carbazole moiety, and the next excited state involves a $\pi-\pi^*$ transition centred on the terpyridine unit. In particular, this is perfectly fulfilled for dyads equipped with a relatively short bridge (*i.e.*, **1–4**), while it becomes more complicated for **5** and **6**, due to the presence of low-lying π and π^* orbitals centered on the highly conjugated bridge. As a consequence, intruder CT states centered on the bridging unit are found in **5** and **6** (Tables S12 and S13).

The situation is totally different for dyad **7**, in which the two lowest-energy excitations are localized on the ethynyl-anthracene unit (see above), while the local excitations on the carbazole moiety and on the terpyridine are associated to the $S_0 \rightarrow S_5$ and $S_0 \rightarrow S_6$ transitions, respectively (Table S14).

Notably, the CT vertical excitation (*i.e.*, $S_0 \rightarrow S_1$ in **1–6**) is not a through-space transition involving the π orbitals of the carbazole donor and the π^* orbitals of the terpyridine acceptor. As a consequence, the mutual position of these two terminal moieties has virtually no effect on the absorption properties of these dyads. This is the reason why, also in this case, no substantial differences were noticed when set of analogous conformers are compared (*i.e.*, differences in excitation energy well below 0.01 eV and associated oscillator strength within $\pm 5\%$).

By comparing the electron densities of the ground-state and of the S_1 CT state, according to the method described by Ciofini *et al.*,^[61,62] it is possible to quantitatively evaluate that the barycenters of the spatial regions of positive and negative charge are not centered on the carbazole and terpyridine units, but are located along the two sides of the bridge (Figure S7). In Table 1 are reported the distance between such barycentres (D_{CT}) for all the dyads and it can be clearly observed that the D_{CT} value is always well below the actual distance of the carbazole-donor and the terpyridine-acceptor groups (see D_{CT}/d_{DA} in Table 1). Moreover, the degree of charge-separation of the S_1 CT state decreases with the bridge length, confirming that the higher the π -conjugation of the bridging moiety, the higher the localization of the CT state on that unit, as already observed for other push-pull dyads.^[61]

In agreement with experimental data, the $S_0 \rightarrow S_1$ vertical excitations of dyad **1** and **3** are the most blue-shifted of the series and are estimated to be almost isoenergetic (Table 1 and Figure 2). The addition of one ethynyl spacer in the bridging unit induces a red shift of about 0.36 eV in the CT transition, as observed when passing from **1** (and **3**) to **4** (and **5**). This finding is also confirmed by spectral data and is mainly due to LUMO stabilization (Figure 1). Finally, the $S_0 \rightarrow S_1$ transition computed for dyad **6** is the most red-shifted of the series and a further stabilization of the corresponding CT state is observed with respect to **4** and **5**. This

stabilization is confirmed by experimental findings (*i.e.*, 0.20 vs. 0.15 eV, respectively).

Emission properties

The fluorescence spectra of **1–7** are reported in Figure 3 both in toluene (full lines) and in dimethylformamide solutions (dashed lines). In contrast to what observed for absorption spectra, the emission properties of the dyads are strongly affected by the polarity of the solvent and very pronounced red-shifts are generally observed when moving from toluene to the more polar dimethylformamide solvent (Figure 3). This finding underpins the CT nature of the emitting states, as already anticipated in the previous section and in our earlier work.^[49]

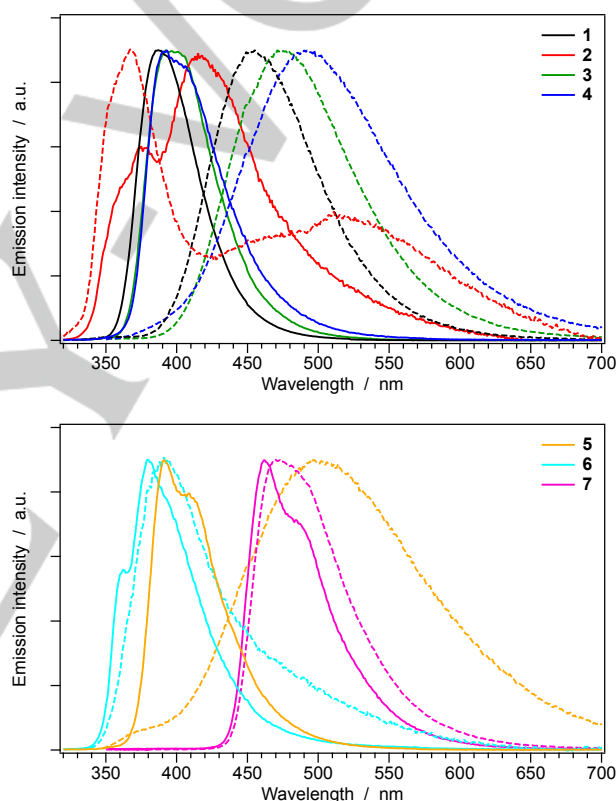


Figure 3. Normalized fluorescence spectra of **1–7** in toluene (full lines) and dimethylformamide (dashed lines) at 298 K.

In toluene, the emission properties of **3**, **4** and **5** are very similar to that of the simplest dyad **1**, which has carbazole moiety directly attached to the 4'-phenyl-terpyridine one. In fact, all of these compounds exhibit a relatively unstructured emission band centred at around 400 nm and display high photoluminescence quantum yields (PLQYs, ranging between 50 and 70%) with similar radiative and non-radiative decay constants (*i.e.*, $k_r \approx k_{nr} \approx 4 \cdot 10^8 \text{ s}^{-1}$), as summarized in Table 2.

On the contrary, in polar dimethylformamide media, the emission spectra of these dyads are strongly red-shifted compared to toluene and are no longer superimposable to one another (Table

FULL PAPER

2 and Figure 3). In fact, the bathochromic shift of the emission maximum is more pronounced for the dyads having longer bridges separating the carbazole and terpyridine units, as clearly validated by the trend: $1 < 3 < 4 < 5$, with emission maxima of 453, 475, 495 and 502 nm, respectively (Table 2).

Moreover, it is worth noting that the radiative and non-radiative rate constant are lower in DMF (*i.e.*, $k_r \approx k_{nr} \approx 1 \cdot 10^8 \text{ s}^{-1}$) since the singlet lifetimes are substantially longer compared to toluene, while the PLQYs do not strongly change (Table 2).

Table 2. Luminescence properties and excited state lifetimes of the donor-acceptor dyads.

	Toluene, 298 K			DMF, 298 K			Bu-CN, 77 K	
	λ_{max} [nm]	PLQY [%]	τ [ns]	λ_{max} [nm]	PLQY [%]	τ [ns]	λ_{max} [nm]	τ [ns]
1	386	62.8	2.1	453	55.0	6.1	380	2.2
2	375, 415	1.6	[a]	365, 510	0.8	[a]	383	1.2
3	392, 400 ^{sh}	66.0	1.2	475	70.9	3.9	384	1.8
4	390, 406 ^{sh}	50.1	1.0	495	44.3	4.0	403	1.1
5	390, 407 ^{sh}	68.5	0.8	502	45.6	3.8	390	0.8
6	380	6.3	[b]	391, 490 ^{sh}	5.2	[b]	400	0.7
7	462, 483 ^{sh}	60.1	2.4	475	57.3	2.6	458, 485	2.7

[a] Bi-exponential lifetime, see ref.^[49] for further details. [b] Bi-exponential lifetime with two components: 0.8 ns (predominant at shorter wavelengths) and 0.5 ns (at longer wavelengths).

A more complicated excited-state scenario is observed in the case of **2** and **6** (*i.e.*, the only dyads having an ethynyl spacer directly linked to the carbazole donor moiety), since multiple emission features are observed in both toluene and dimethylformamide solutions (Figure 3). Such dual emissions are attributed to the presence of two excited-state conformers, as we already pointed out in our earlier work for dyad **2**.^[49] The rather structured emission band around 380 nm is attributed to the fluorescence of a local-excited (LE) state, centered on the carbazole unit (see below); on the contrary, the emission at longer wavelengths arises from a CT state, which is particularly stabilized in polar media (Figure 3). Notably, the fluorescence quantum yields of **2** and **6** are over 50 times smaller than those of the other dyads, suggesting the presence of effective non-radiative deactivation pathways to the ground state, due to the presence of accessible dark states leading to S_1/S_0 conical intersections (see below).

The case of dyad **7** is completely different, as no CT bands are detected in any solvent and only the fluorescence of the anthracene unit is recorded in both solvents ($\lambda_{\text{max}} \approx 460 \text{ nm}$, Table 2 and Figure 3). Accordingly, such emission band resembles that of other phenylethynyl-anthracene derivatives^[56] and it is virtually

not affected by the solvent polarity. As a matter of fact, the anthracene moiety incorporated in the bridge serves as the final sink of the excitation energy.

The emission properties of all the dyads were also investigated in butyronitrile glass at 77 K (Figure 4 and Table 2). Under these conditions, the geometrical relaxation of the excited states is highly prevented and solvent reorganization effects are drastically reduced. Therefore, all the emission profiles are similar to those recorded in the most apolar liquid medium (*i.e.*, toluene), as it can be inferred by comparing Figure 4 and 3.

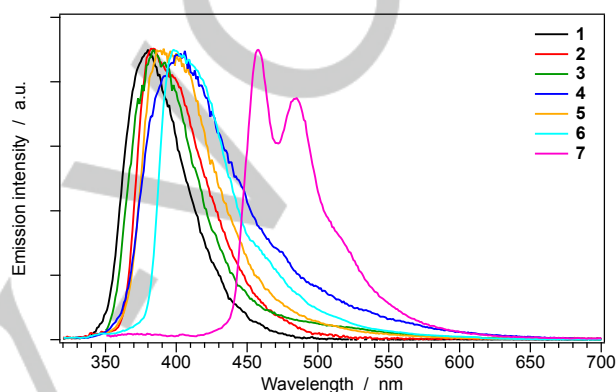


Figure 4. Normalized fluorescence spectra of **1–7** in butyronitrile glass at 77 K.

It is also worth mentioning that, at 77 K, the population of thermally-accessible locally-excited states is nearly suppressed, leading to the emission only from the lower-lying CT minimum. As a consequence, the 77 K fluorescence spectra of **2** and **6** display only the unstructured CT band of the “bright” planar S_1 conformer (see next section) and are largely superimposed with all the other spectral profiles of **1–6**. Not surprisingly, only the spectrum of **7** clearly differs from all the others, but this is simply because its fluorescence is due to the anthracene unit, as already discussed above.

The emission properties were also explored in room-temperature PMMA matrix, at different concentration of the dyads. In Figure S8, the solid-state emission spectra of dyad **3** are reported, as a representative example of the whole series. No substantial differences in the luminescence profiles are observed, if compared to toluene solution, and only a minor red shift is found when increasing the concentration of the dyad (Figure S8).

TD-DFT optimization of the excited states

The nature of the emitting states was further elucidated by the TD-DFT optimization of the lowest excited state of all the investigated molecules. Upon S_1 relaxation, all the dyads displaying a CT emission (*i.e.*, **1–6**) undergo a substantial planarization, which is due to the population of a quinoid-like π^* orbital mainly localized on the bridging unit (Tables S15–S21). For the short-bridged dyads (*i.e.*, **1** and **2**), this planarization mainly entails the dihedral angle between the terpyridine unit and the nearby phenyl moiety

FULL PAPER

of the bridge (*i.e.*, angle θ_1 in Tables S1 and S2). On the contrary, the flattening starts to mainly involve the bridge for dyads with longer spacers (Tables S3–S6 and S17–20).

Such flattening relaxations are able to strongly stabilize the S_1 CT state, resulting in large Stoke shifts, as also found experimentally (compare Figure 2 and 3). The CT emission of dyad **1**, computed using state-specific solvation,^[63,64] is estimated to occur at 384 nm (in excellent agreement with experimental data, see Table 2), and it is the most blue-shifted of the series. When the bridge length is increased, a gradual red-shift of the CT emission is observed (up to 0.45 eV). Finally, the anthracene-centred S_1 minimum of dyad **7** is computed to be 2.45 eV above S_0 (*i.e.*, 506 nm).

TD-DFT S_1 optimizations were also carried out in dimethylformamide, but no substantial differences were detected with respect to toluene, as far as the nature of the emitting state is concerned. On the contrary, a red-shift of about (0.43 ± 0.11) eV is estimated for the emission of dyads **1–6**, basically due to mere solvation effects. This is in line with the experimentally observed red-shift of (0.64 ± 0.07) eV (Table 2).

To get a deeper insight of the far lower PLQYs of **2** and **6** with respect to the other dyads of the series (Table 2), we considered that the rotation of the carbazole moiety around the C=C bridging spacer is practically barrierless (Figure S3), so that the perpendicular conformers of **2** and **6** are also populated at 298 K (*e.g.*, the relative population of the perpendicular and co-planar conformers of **2** is 0.4 vs. 0.6, respectively). When the ethynyl-carbazole moiety is orthogonal to the rest of the bridge, a slight increase in the energy of the $S_0 \rightarrow S_1$ transition is observed, with a substantial decrease in the associated oscillator strength (compare Table S9 and S22 for dyad **2** in toluene).^[49] Such transition preserves the same CT nature as in the co-planar conformers and is basically a $\pi-\pi^*$ excitation, but the π and the π^* molecular orbitals associated with such excitation are now perpendicular to each other (Table S22). As a consequence, the relaxation of such CT state leads to a TS with C_2 symmetry and an imaginary frequency of 278 cm^{-1} (Figure 5, top), which evolves toward a low-lying trans-bent $\pi-\sigma^*$ state with broken symmetry (Figure 5, bottom).

This excited-state scenario, in which both a linear “bright” $\pi-\pi^*$ state and a trans-bent “dark” $\pi-\sigma^*$ state are located on the S_1 potential energy surface, resembles those already investigated for diphenylacetylene^[52,65] and for other organic molecules with C≡X (X = C or N) groups.^[66] However, in the present case, we did not succeed in finding a minimum for the trans-bent $\pi-\sigma^*$ state of **2** since TD-DFT optimizations failed. In fact, upon geometry relaxation, this $\pi-\sigma^*$ state rapidly approaches S_0 (*i.e.*, the optimization failed with S_1 being only 0.54 eV above S_0), suggesting the presence of a peaked S_1/S_0 conical intersection, which could be responsible for the strong luminescence quenching in this type of dyads.

Indeed, also highly emitting dyads **4** and **5** are equipped with a bridge having a tolane-like moiety, so that the presence of dark $\pi-\sigma^*$ states could be potentially feasible upon $S_0 \rightarrow S_1$ excitation and responsible for an emission quenching. However, TD-DFT optimizations of the twisted S_1 CT state of **4** (starting from conformers having the diphenyl-acetylene moiety in the pseudo-

D_{2d} orthogonal conformation) lead to molecular planarization and to the same highly-emissive $\pi-\pi^*$ S_1 minima already described for the “standard” conformers of **4** (Table S4 and S18).

These theoretical findings are able to rationalize why only dyads having the ethynyl spacer directly linked to the carbazole moiety (*i.e.*, **2** and **6**) display a significant emission quenching, while the presence of the ethynyl group in other parts of the dyad bridge does not cause any appreciable reduction in the PLQYs (Table 2).

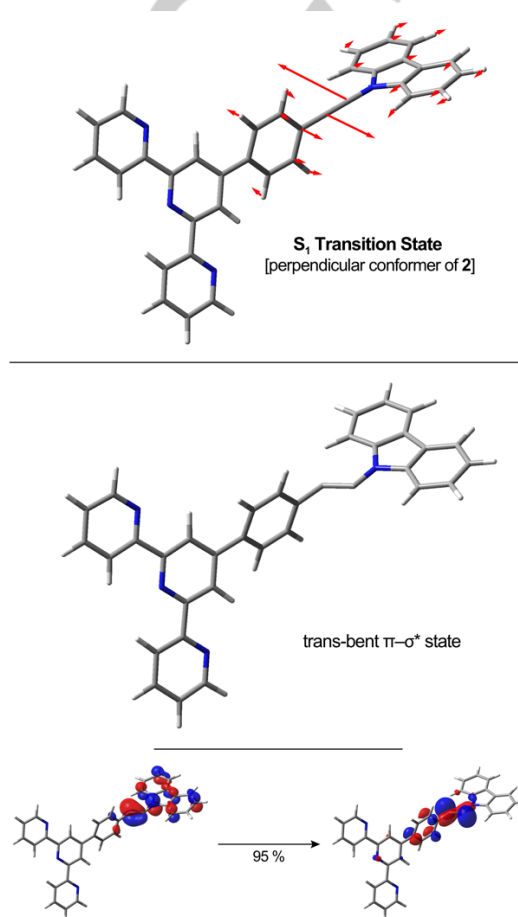


Figure 5. (Top) Transition state (TS) on the S_1 potential-energy surface of the perpendicular conformer of dyad **2**; the displacement vectors associated to its imaginary frequency are also reported. (Bottom) Last point of the failed optimization of the $\pi-\sigma^*$ state, obtained by following the imaginary frequency of the above-mentioned TS (at this geometry, S_1 is only 0.54 eV above S_0); the orbitals contributing to such $S_0 \rightarrow S_1$ excitation are also reported. Calculations are carried out in toluene at the TD-M06-2X/6-31+G(d) level of theory.

Conclusions

New luminescent organic systems to be used for optoelectronic applications require careful synthetic design and a thorough rationalization of structure-property relationships by means of advanced theoretical tools. In this work, we have designed, synthesized and examined in detail D- π -A systems where carbazole (D) and terpyridine (A) moieties are connected through

FULL PAPER

organic π -conjugated bridges of different length, connectivity and structure, the latter including ethynyl, phenylene, and anthracenyl groups (**1-7**). Effect of solvent polarity have been also examined. All of the individual subunits in **1-7** are virtually free to rotate along the molecular backbone at room temperature, except when the carbazole moiety is linked directly to a phenyl unit. The absorption spectra of **1-7** exhibit fairly negligible solvatochromic effects and very minor changes on the addition of phenylene groups directly attached to the carbazole donor (see e.g., **2** vs. **4**). On the contrary, when the carbazole donor is connected to an ethynyl group, some red spectral shift is observed (see e.g., **1** vs. **2**). **7** is a substantially different case with the characteristic absorption and emission features of the anthracene moiety, which turns out to be the lowest energy subunit within the molecular architecture. **1-6** are characterized by charge-transfer solvatochromic emissions with high PLQY (≈ 45 -70%), except when an ethynyl group is attached directly to the carbazole unit. In this case, the emission bands are broadened and much weaker (PLQY ≈ 1 -6%), due to the presence of thermally-accessible trans-bent non emissive π - σ^* excited states. DFT calculations have enabled a full rationalization of the photophysical properties, in relation to structural and electronic peculiarities of each investigated dyad. The results presented here provide a deeper insight of structure-activity relationships of these D- π -A systems, widening the possibility to rationally design and prepare carbazole-terpyridine chromophores and luminophores with tailored photophysical properties, to be potentially used for optoelectronic applications.

Experimental Section

Materials. Analytical grade solvents and commercially available reagents were used as received, unless otherwise stated. 4-Bromobenzaldehyde (**8**), 9H-Carbazole-9-(4-phenyl) boronic acid pinacol ester (**10**), 1-Bromo-4-iodobenzene (**11**), 4-Ethynylbenzaldehyde (**13**), (4-Bromophenylethynyl)trimethylsilane (**17**), 9,10-Dibromoanthracene (**21**), 2-acetylpyridine, carbazole were commercially available (Sigma Aldrich). Chromatographic purifications were performed using 70-230 mesh silica or aluminum oxide. Solvents were dried and distilled according to standard procedure and stored under nitrogen. Compounds 4'-[*p*-(Carbazole-9-yl)phenyl]-2,2':6',2''-terpyridine^[43] (**1**) and 4'-[4-(9H-Carbazol-9-ylethynyl)phenyl]-2,2':6',2''-terpyridine^[49] (**2**), used in the present investigation, were prepared according to reported methods.

General information. ¹H, ¹³C, NMR spectra were recorded on a Varian Inova (300 and 600 MHz for ¹H) or on a Varian Mercury (400 MHz for ¹H) spectrometer. Chemical shifts (δ) are reported in ppm relative to residual solvent signals for ¹H and ¹³C NMR (¹H NMR: 7.26 ppm for CDCl₃; ¹³C NMR: 77.0 ppm for CDCl₃). ¹³C NMR spectra were acquired with ¹H broad band decoupled mode. Coupling constants are given in Hz. The high-resolution mass spectra (HRMS) were obtained with an ESI-QTOF (Agilent Technologies, model G6520A) instrument and the *m/z* values are referred to the monoisotopic mass. ESI-MS analyses were performed by direct injection of methanol or water-acetonitrile solutions of the compounds using a WATERS ZQ 4000 mass spectrometer.

Synthesis of 9-(4'-([2,2':6',2''-terpyridin]-4'-yl)-[1,1'-biphenyl]-4-yl)-9H-carbazole (3**).**

4'-(4-bromophenyl)-2,2':6',2''-terpyridine (**9**) was prepared according to a

modification of a reported method.^[40] 2-Acetylpyridine (1.3 mL, 12 mmol) was added to a stirred suspension of crushed NaOH (480.0 mg, 12 mmol) in PEG 200 (10 mL) at 0° C. After 30 minutes 4-bromobenzaldehyde (**8**) (925.1 mg, 5 mmol) was added and stirring was continued at 0° C for 2 h. Then a concentrated aqueous NH₃ solution (15.0 mL) was added and the suspension stirred at 100° C for 24 h. The precipitate was isolated by vacuum filtration and washed with water (50 mL) and ethanol (10 mL) to give product (**9**) as a white solid in 73% yield (1.42 g). Spectral data were consistent with the literature.^[40]

9-(4-(4,4,5,5-tetramethyl-1,3,2-dioxaborolan-2-yl)phenyl)-9H-carbazole (**10**) (184.6 mg, 0.5 mmol), ethanol (63 μ L) and K₂CO₃ (2M in water, 250 μ L, 0.5 mmol) were added to a solution of 4'-(4-bromophenyl)-2,2':6',2''-terpyridine (**9**) (194.5 mg, 0.5 mmol) in anhydrous THF (1.5 mL) under nitrogen atmosphere. The solution was degassed with nitrogen and after 10 minutes Pd(PPh₃)₄ (17.3 mg, 0.015 mmol) was added and the solution stirred at 70° C overnight. When the reaction was terminated, the solvent was evaporated, distilled water was added and the resultant solution was extracted with dichloromethane (3 x 15 mL). The collected organic layer was dried over anhydrous MgSO₄ and then evaporated. The residue was purified by alumina column chromatography using a mixture of CH₂Cl₂/MeOH (98:2) to give product (**3**) as a white solid in 25% yield (69.3 mg). ¹H NMR (CD₃Cl, 400 MHz) δ 8.86 (s, 2H), 8.78 (d, *J* = 4.8 Hz, 2H), 8.72 (d, *J* = 8.0 Hz, 2H), 8.09 (d, *J* = 8.8 Hz, 2H), 7.96-7.89 (m, 4H), 7.86 (d, *J* = 8.8 Hz, 2H), 7.69 (d, *J* = 8.0 Hz, 2H), 7.51 (d, *J* = 8.0 Hz, 2H), 7.47-7.37 (m, 4H), 7.32 (dt, *J*_t = 8.0 Hz, *J*_d = 1.1 Hz, 2H); ¹³C NMR (CD₃Cl, 100 MHz) δ 156.0 (C), 149.7 (C), 149.0 (CH), 141.4 (C), 140.9 (C), 140.8 (C), 139.4 (C), 137.6 (C), 137.2 (CH), 137.2 (C), 128.5 (CH), 127.9 (CH), 127.6 (CH), 127.4 (CH), 126.0 (CH), 124.0 (CH), 123.5 (C), 121.5 (CH), 120.3 (CH), 120.0 (CH), 118.9 (CH), 109.8 (CH); HRMS (ESI-QTOF) *m/z*: calcd. for C₃₉H₂₇N₄⁺: 551.2230; found 551.2224 (M+H)⁺; ESI-MS: 551 [M⁺ + 1].

Synthesis of 9-(4-(4'-([2,2':6',2''-terpyridin]-4'-yl)phenyl)ethynyl)phenyl)-9H-carbazole (4**).**

9-(4-bromophenyl)-9H-carbazole (**12**) was prepared according to a modification of a reported method.^[50] Carbazole (200 mg, 1.2 mmol), Cs₂CO₃ (325.8 mg, 1.2 mmol), CuI (22.8 mg, 0.12 mmol) and LiCl (50.7 mg, 1.2 mmol) were added to a solution of 1-bromo-4-iodobenzene (**11**) (372 mg, 1.32 mmol) in DMF (7 mL), and the resulting mixture was stirred at 150° C for 48 hours. Eventually, water was added and the mixture was extracted with ethyl acetate (5 x 10 mL). The organic phase was then washed with brine, dried over Na₂SO₄ and the solvent evaporated. The residue was purified by silica gel column chromatography using hexane as eluent, to give product **12** as a pale-yellow solid in 71% yield (272.9 mg). Spectral data were consistent with the literature.^[50]

In a Schlenk flask, **13** (132.2 mg, 1.02 mmol), Pd(PPh₃)₂Cl₂ (59.4 mg, 0.08 mmol) and CuI (16.2 mg, 0.08 mmol) were added to a solution of **12** (272.9 mg, 0.85 mmol) in TEA (7 mL) and toluene (1 mL); the solution was then stirred under nitrogen atmosphere for 24 hours at 50° C. The progress of the reaction was monitored using TLC analysis on silica gel petroleum ether / dichloromethane (2:1). Upon completion, water was added and the resulting mixture was extracted with dichloromethane (3 x 10 mL). The combined organic phase was then washed with HCl 1M (1 x 10 mL), brine and dried over Na₂SO₄. Solvent was evaporated and the residue was purified by silica gel column chromatography using a mixture of dichloromethane / petroleum ether (2:8) to give 4-(4-(9H-carbazol-9-yl)phenyl)ethynylbenzaldehyde (**14**) as a pale white solid in 22% yield (67.6 mg). Spectral data were consistent with the literature.^[67]

2-Acetylpyridine (50 μ L, 0.42 mmol) was added to a stirred suspension of crushed NaOH (16.7 mg, 0.42 mmol) in PEG 200 (0.5 mL) at 0° C. After 30 minutes 4-(4-(9H-carbazol-9-yl)phenyl)ethynylbenzaldehyde (**14**) (67.6 mg, 0.21 mmol) was added and stirring was continued at 0° C for 2 h. Then concentrated aqueous NH₃ solution (0.7 mL) was added and the suspension stirred at 100° C for 24 h. Eventually, water was added and the mixture was extracted with dichloromethane (3 x 10 mL). The organic

FULL PAPER

phase was then washed with brine, dried over Na_2SO_4 . Solvent was evaporated and methanol was added. The precipitate solid was collected by vacuum filtration and washed with water (50 mL) and ethanol (10 mL) to give product (**4**) as a white solid in 35% yield (41.2 mg). $^1\text{H NMR}$ (CD_3Cl , 400 MHz) δ 8.82 (s, 2H), 8.77 (d, $J = 4.4$ Hz, 2H), 8.72 (d, $J = 8.0$ Hz, 2H), 8.16 (d, $J = 8.0$ Hz, 2H), 7.98 (d, $J = 8.0$ Hz, 2H), 7.93 (t, $J = 8.0$ Hz, 2H), 7.81 (d, $J = 8.0$ Hz, 4H), 7.74 (d, $J = 8.0$ Hz, 2H), 7.61 (d, $J = 8.0$ Hz, 2H), 7.50-7.38 (m, 6H) 7.31 (t, $J = 7.6$ Hz, 2H); $^{13}\text{C NMR}$ (CD_3Cl , 100 MHz) δ 156.0 (C), 155.9 (C), 149.4 (C), 149.0 (CH), 140.6 (C), 138.4 (C), 137.7 (C), 137.1 (CH), 133.2 (CH), 132.3 (CH), 127.4 (CH), 126.9 (CH), 126.1 (CH), 124.0 (CH), 123.8 (C), 123.6 (C), 122.1 (C), 121.5 (CH), 120.4 (CH), 120.2 (CH), 118.8 (CH), 109.8 (CH), 90.2 (C_{alk}), 90.1 (C_{alk}); HRMS (ESI-QTOF) m/z : calcd. for $\text{C}_{41}\text{H}_{27}\text{N}_4^+$: 575.2231; found 575.2227 (M+H) $^+$; ESI-MS: 575 [$\text{M}^+ + 1$], 597 [$\text{M}^+ + \text{Na}$], 607 [$\text{M}^+ + \text{MeOH}$].

Synthesis of 9-(4'-((4-([2,2':6',2''-terpyridin]-4'-yl)phenyl)ethynyl)-[1,1'-biphenyl]-4-yl)-9H-carbazole (**5**).

4-((4-bromophenyl)ethynyl)benzaldehyde (**15**) was prepared according to the modification of a reported method.^[68] In a Schlenk flask, **13** (106.5 mg, 0.82 mmol), $\text{Pd}(\text{PPh}_3)_2\text{Cl}_2$ (10.9 mg, 0.02 mmol) and CuI (15.7 mg, 0.03 mmol) were added to a solution of 1-bromo-4-iodobenzene (**11**) (276.1 mg, 0.98 mmol) in TEA (8 mL); the solution was then stirred under nitrogen atmosphere for 24 hours at room temperature. The progress of the reaction was monitored using TLC analysis on silica gel petroleum ether / ethyl acetate (9:1). Upon completion, water was added and pH was adjusted to 5 using HCl 1M. The resulting mixture was extracted with dichloromethane (3 x 10 mL). The combined organic phase was then washed with brine and dried over Na_2SO_4 . Solvent was evaporated and the residue was purified by silica gel column chromatography using a mixture of ethyl acetate / petroleum ether (2:98) to give product **15** as a pale-yellow solid in 94% yield (265.2 mg). Spectral data were consistent with the literature.^[68]

2-Acetylpyridine (222 μL , 1.98 mmol) was added to a stirred suspension of crushed KOH (110.9 mg, 1.98 mmol) in ethanol (5 mL). After 30 minutes 4-((4-bromophenyl)ethynyl)benzaldehyde (**15**) (281.2 mg, 0.99 mmol) was added and stirring was continued for 2 h. Then concentrated aqueous NH_3 solution (1 mL) was added and the suspension stirred at 100°C for 24 h. Eventually, water was added and the mixture was extracted with dichloromethane (3 x 10 mL). The organic phase was then washed with brine and dried over Na_2SO_4 . Solvent was evaporated and methanol was added. The precipitate solid was collected by vacuum filtration and washed with water (10 mL) and methanol (10 mL) to give 4'-((4-bromophenyl)ethynyl)phenyl)-2,2':6',2''-terpyridine (**16**) as a brown solid in 15% yield (71.0 mg). $^1\text{H NMR}$ (CD_3Cl , 300 MHz) δ 8.76 (s, 2H), 8.74 (dq, $J_a = 4.8$ Hz, $J_d = 0.9$ Hz, 2H), 8.68 (dt, $J_t = 8.1$ Hz, $J_d = 1.1$ Hz, 2H), 7.94-7.86 (m, 4H), 7.67 (d, $J = 8.4$ Hz, 2H), 7.51 (d, $J = 8.4$ Hz, 2H), 7.43 (d, $J = 8.4$ Hz, 2H), 7.40 (ddd, $J = 7.5$ Hz, $J = 4.8$ Hz, $J = 1.2$ Hz, 2H); $^{13}\text{C NMR}$ (CDCl_3 , 100 MHz) δ 156.1 (C), 156.0 (C), 149.3 (C), 149.1 (CH), 138.4 (C), 136.9 (CH), 133.1 (CH), 132.1 (CH), 131.7 (CH), 127.3 (CH), 123.9 (CH), 123.6 (C), 122.7 (C), 122.1 (C), 121.4 (CH), 118.6 (CH), 90.2 (C_{alk}), 89.7 (C_{alk}).

9-(4-(4,4,5,5-tetramethyl-1,3,2-dioxaborolan-2-yl)phenyl)-9H-carbazole (**10**) (30.3 mg, 0.08 mmol), ethanol (0.1 mL) and K_2CO_3 (2M in water, 41 μL , 0.08 mmol) were added to a solution of 4'-((4-bromophenyl)ethynyl)phenyl)-2,2':6',2''-terpyridine (**16**) (40.0 mg, 0.08 mmol) in THF (0.5 mL) under nitrogen atmosphere. The solution was degassed with nitrogen and after 10 minutes $\text{Pd}(\text{PPh}_3)_4$ (2.8 mg, 0.002 mmol) was added and the solution stirred at 70°C overnight. When the reaction was terminated the solvent was evaporated, distilled water was added, and the resultant solution was extracted with dichloromethane (3 x 15 mL). The collected organic layer was dried over anhydrous Na_2SO_4 and then evaporated. The residue was purified by silica gel column chromatography using a mixture of dichloromethane / methanol (99:1), and the resulting fractions were concentrated and the residue dissolved in

dichloromethane and washed with methanol. Product (**5**) was collected by filtration of the solution as a white solid in 30% yield (16.2 mg). $^1\text{H NMR}$ (CDCl_3 , 400 MHz) δ 8.78 (s, 2H), 8.76 (d, $J = 4.0$ Hz, 2H), 8.70 (d, $J = 8.0$ Hz, 2H), 8.17 (d, $J = 8.0$ Hz, 2H), 7.95 (d, $J = 8.4$ Hz, 2H), 7.90 (dt, $J_1 = 1.6$ Hz, $J_2 = 7.6$ Hz, 2H), 7.86 (d, $J = 8.4$ Hz, 2H), 7.74-7.70 (m, 4H), 7.67 (d, $J = 8.4$ Hz, 2H), 7.51-7.41 (m, 4H), 7.38 (dd, $J_1 = 4.8$ Hz, $J_2 = 7.0$ Hz, 2H), 7.31 (t, $J = 7.0$ Hz, 2H); $^{13}\text{C NMR}$ (CDCl_3 , 100 MHz) δ 156.1 (C), 156.0 (C), 149.4 (C), 149.1 (CH), 140.8 (C), 140.1 (C), 139.3 (C), 138.2 (C), 137.2 (C), 137.0 (CH), 132.3 (CH), 132.2 (CH), 128.4 (CH), 127.4 (CH), 127.3 (CH), 127.0 (CH), 126.0 (CH), 124.0 (C), 123.9 (CH), 123.5 (C), 122.4 (C), 121.4 (CH), 120.3 (CH), 120.0 (CH), 118.7 (CH), 109.8 (CH), 90.7 (C_{alk}), 90.1 (C_{alk}); HRMS (ESI-QTOF) m/z : calcd. for $\text{C}_{47}\text{H}_{31}\text{N}_4^+$: 651.2543; found 651.2540 (M+H) $^+$; ESI-MS: 651 [$\text{M}^+ + 1$].

Synthesis of 9-((4-((4-([2,2':6',2''-terpyridin]-4'-yl)phenyl)ethynyl)phenyl)ethynyl)-9H-carbazole (**6**).

In a Schlenk flask, $\text{Pd}(\text{PPh}_3)_2\text{Cl}_2$ (40.3 mg, 0.06 mmol) and CuI (11.0 mg, 0.06 mmol) were added to a solution of ((4-bromophenyl)ethynyl)trimethylsilane (**17**) (291.1 mg, 1.15 mmol) in TEA (3 mL) and toluene (1 mL), **13** (164.4 mg, 1.26 mmol); the solution was then stirred under nitrogen atmosphere for 3 hours at 50°C. The progress of the reaction was monitored using TLC analysis on silica gel petroleum ether / ethyl acetate (2:1). Upon completion, water was added and the resulting mixture was extracted with dichloromethane (3 x 10 mL). The combined organic phase was then washed with HCl 1M (1 x 10 mL), brine and dried over Na_2SO_4 . Solvent was evaporated and the residue was purified by silica gel column chromatography using a mixture of ethyl acetate / petroleum ether (2:98) to give 4-((4-((trimethylsilyl)ethynyl)phenyl)ethynyl)benzaldehyde (**18**) as a pale-yellow solid in 44% yield (150.2 mg). Spectral data were consistent with the literature.^[69]

Compound **18** (117.5 mg, 0.39 mmol) and AgF (49.3 mg, 0.39 mmol) were dissolved in acetonitrile (10 mL). The reaction flask was wrapped in aluminium foil and NBS (69.2 mg, 0.39 mmol) was added. The mixture was stirred overnight at room temperature. Then the solid was filtered off and washed with acetonitrile (10 mL). The solution was evaporated and the resulting residue was dissolved in ethylic ether and washed with water (3 x 25 mL). The organic part was dried on anhydrous Na_2SO_4 and then evaporated to give product 4-((4-(bromoethynyl)phenyl)ethynyl)benzaldehyde (**19**) as a white solid in 78% yield (93.2 mg). $^1\text{H NMR}$ (CD_3Cl , 300 MHz) δ 10.02 (s, 1H), 8.87 (d, $J = 8.4$ Hz, 2H), 7.67 (d, $J = 8.4$ Hz, 2H), 7.49 (d, $J = 8.4$ Hz, 2H), 7.44 (d, $J = 8.4$ Hz, 2H).

Carbazole (45.9 mg, 0.27 mmol), K_3PO_4 (116.5 mg, 0.55 mmol), $\text{CuSO}_4 \cdot 5\text{H}_2\text{O}$ (13.7 mg, 0.06 mmol) and 1,10-phenanthroline (19.8 mg, 0.11 mmol) were added to a solution of 4-((4-(bromoethynyl)phenyl)ethynyl)benzaldehyde (**19**) (93.2 mg, 0.30 mmol) in anhydrous THF (7 mL). The reaction mixture was purged with nitrogen and heated at 70°C for 5 days. The progress of the reaction was monitored using TLC analysis. Upon completion, the reaction mixture was dried *in vacuo* and the residue was dissolved in water and extracted with dichloromethane (3 x 15 mL). The combined organic phases were dried with anhydrous Na_2SO_4 and then evaporated. The crude residue was purified on silica gel flash chromatography using a mixture of hexane / ethyl acetate (95:5) to give 4-((4-((9H-carbazol-9-yl)ethynyl)phenyl)ethynyl)benzaldehyde (**20**) as a pale-yellow solid in 47% yield (55.8 mg). $^1\text{H NMR}$ (CD_3Cl , 400 MHz) δ 10.04 (s, 1H), 8.06 (d, $J = 8.4$ Hz, 2H), 7.89 (d, $J = 8.4$ Hz, 2H), 7.74 (d, $J = 8.4$ Hz, 2H), 7.70 (d, $J = 8.4$ Hz, 2H), 7.59-7.50 (m, 2H), 7.45-7.35 (m, 2H), 7.28-7.21 (m, 4H).

2-Acetylpyridine (50 μL , 0.42 mmol) was added to a stirred suspension of crushed NaOH (17.2 mg, 0.42 mmol) in PEG 200 (1.5 mL) at 0°C. After 30 minutes, **20** (55.8 mg, 0.14 mmol) was added and stirring was continued at 0°C for 2 h. Then a concentrated aqueous NH_3 solution (1.5 mL) was added and the suspension stirred at 100°C for 24 h. After this time water was added and the mixture was extracted with dichloromethane (3 x 10 mL). The organic phase was then washed with brine and dried over

FULL PAPER

Na₂SO₄. Solvent was evaporated and methanol was added. The precipitate solid was collected by vacuum filtration and washed with water (50 mL) and ethanol (10 mL) to give product (**6**) as a pale-yellow solid in 15% yield (12.6 mg). ¹H NMR (CD₃Cl, 400 MHz) δ 8.77 (s, 2H), 8.75 (dq, *J*_q = 4.8 Hz, *J*_d = 1.0 Hz, 2H), 8.69 (dt, *J*_t = 8.0 Hz, *J*_d = 1.0 Hz, 2H), 8.05 (d, *J* = 8.0 Hz, 2H), 7.94 (d, *J* = 8.4 Hz, 2H), 7.74 (d, *J* = 8.0 Hz, 2H), 7.70 (d, *J* = 8.0 Hz, 4H), 7.61 (d, *J* = 1.6 Hz, 4H), 7.55 (dt, *J*_t = 7.6 Hz, *J*_d = 1.1 Hz, 2H), 7.37 (t, *J* = 6.8 Hz, 4H); ¹³C NMR (CD₃Cl, 100 MHz) δ 156.2 (C), 156.1 (C), 149.4 (C), 149.2 (CH), 140.3 (C), 138.4 (C), 136.9 (CH), 132.2 (CH), 131.7 (CH), 131.1 (CH), 127.3 (CH), 126.8 (CH), 123.9 (C), 123.8 (CH), 123.7 (C), 123.0 (C), 122.4 (C), 122.2 (CH), 121.4 (CH), 120.4 (CH), 118.7 (CH), 111.3 (CH), 90.8 (C_{alk}), 90.6 (C_{alk}), 80.9 (C_{alk}), 74.7 (C_{alk}); HRMS (ESI-QTOF) *m/z*: calcd. for C₄₃H₂₇N₄⁺: 599.2231; found 599.2229 (M+H)⁺.

Synthesis of 9-(4-(10-((2,2':6',2''-terpyridin)-4'-yl)phenyl)ethynyl)anthracen-9-yl)phenyl)-9H-carbazole (**7**).

In a Schlenk flask, **13** (249.6 mg, 1.92 mmol), TEA (0.5 mL), Pd(PPh₃)₂Cl₂ (28.0 mg, 0.04 mmol) and CuI (19.1 mg, 0.10 mmol) were added to a solution of 9,10-dibromoanthracene (**21**) (645.2 mg, 1.92 mmol) in DMF (10 mL) and 1,4-dioxane (4 mL); the solution was then stirred under nitrogen atmosphere for 24 hours at 80°C. The progress of the reaction was monitored using TLC analysis on silica gel petroleum ether / ethyl acetate (9:1). Upon completion, water was added and the resulting mixture was extracted with dichloromethane (3 x 10 mL). The combined organic phase was then washed with HCl 1M (1 x 10 mL), brine and dried over Na₂SO₄. Solvent was evaporated and the residue was purified by silica gel column chromatography using a mixture of petroleum ether / ethyl acetate (95:5) to give product 4-((10-bromoanthracen-9-yl)ethynyl)benzaldehyde (**22**) as a yellow solid in 35% yield (253.2 mg). Spectral data were consistent with the literature.^[70]

Compound **10** (242.7 mg, 0.66 mmol), ethanol (65 μL) and K₂CO₃ (2M in water, 330 μL, 0.66 mmol) were added to a solution of 4-((10-bromoanthracen-9-yl)ethynyl)benzaldehyde (**22**) (253.2 mg, 0.66 mmol) in THF (1.5 mL) under nitrogen atmosphere. The solution was degassed with nitrogen and after 10 minutes Pd(PPh₃)₄ (19.0 mg, 0.02 mmol) was added and the solution stirred at 70°C overnight. After the reaction was terminated the solvent was evaporated, distilled water was added, and the resultant solution was extracted with dichloromethane (3 x 15 mL). The collected organic layer was dried over anhydrous Na₂SO₄ and then evaporated. The residue was purified by silica gel column chromatography using a mixture of dichloromethane / petroleum ether (1:9) to give product 4-((10-(4-(9H-carbazol-9-yl)phenyl)anthracen-9-yl)ethynyl)benzaldehyde (**23**) as a yellow solid in 38% yield (106.9 mg). ¹H NMR (CD₃Cl, 300 MHz) δ 10.10 (s, 1H), 8.77 (d, *J* = 9 Hz, 2H), 8.22 (d, *J* = 7.8 Hz, 2H), 7.98 (dd, *J* = 8.7 Hz, *J* = 12.3 Hz, 4H), 7.88-7.81 (m, 4H), 7.72-7.65 (m, 6H), 7.57-7.48 (m, 4H), 7.36 (dt, *J*_t = 7.5 Hz, *J*_d = 1.0 Hz, 2H); ¹³C NMR (CD₃Cl, 100 MHz) δ 191.4 (CHO), 140.8 (C), 138.3 (C), 137.4 (C), 137.3 (C), 135.6 (C), 132.6 (CH), 132.5 (C), 132.1 (CH), 130.0 (C), 129.9 (C), 129.8 (CH), 127.3 (CH), 126.9 (CH), 126.9 (CH), 126.8 (CH), 126.1 (CH), 126.0 (CH), 123.6 (C), 120.5 (CH), 120.2 (CH), 116.9 (C), 109.9 (CH), 100.2 (C_{alk}), 90.6 (C_{alk}).

2-Acetylpyridine (66 μL, 0.59 mmol) was added to a stirred suspension of crushed NaOH (24.0 mg, 0.59 mmol) in PEG 200 (1.0 mL) at 0°C. After 30 minutes, compound **23** (106.9 mg, 0.20 mmol) was added and stirring was continued at 0°C for 2 h. Then concentrated aqueous NH₃ solution (3 mL) was added and the suspension stirred at 100°C for 24 h. After this time water was added and the mixture was extracted with dichloromethane (3 x 10 mL). The organic phase was then washed with brine, dried over Na₂SO₄. Solvent was evaporated and methanol was added. The precipitate solid was collected by vacuum filtration and washed with water (50 mL) and ethanol (10 mL). Then it was purified by silica gel column chromatography using a mixture of dichloromethane / methanol (95:5) to give product (**7**) as a yellow solid in 15% yield (22.3 mg). ¹H NMR (CD₃Cl,

400 MHz) δ 8.83 (d, *J* = 10.8 Hz, 4H), 8.79 (d, *J* = 4.8 Hz, 2H), 8.72 (d, *J* = 8.0 Hz, 2H), 8.22 (d, *J* = 8.0 Hz, 2H), 8.05 (d, *J* = 8.0 Hz, 2H), 7.96 (d, *J* = 8.0 Hz, 2H), 7.92 (d, *J* = 8.0 Hz, 4H), 7.84 (t, *J* = 8.0 Hz, 4H), 7.69 (t, *J* = 8.4 Hz, 6H), 7.55-7.49 (m, 4H) 7.42-7.34 (m, 4H); ¹³C NMR (CD₃Cl, 100 MHz) δ 156.0 (C), 149.5 (C), 149.1 (CH), 140.8 (C), 138.4 (C), 137.6 (C), 137.5 (C), 137.4 (C), 137.3 (C), 137.1 (CH), 132.7 (CH), 132.4 (C), 132.2 (CH), 130.1 (C), 127.5 (CH), 127.2 (CH), 127.1 (CH), 126.9 (CH), 126.6 (CH), 126.1 (CH), 126.0 (CH), 124.4 (C), 124.0 (CH), 123.6 (C), 121.5 (CH), 120.5 (CH), 120.2 (CH), 118.8 (CH), 117.7 (C), 109.9 (CH), 88.1 (C_{alk}), 77.2 (C_{alk}); HRMS (ESI-QTOF) *m/z*: calcd. for C₅₅H₃₅N₄⁺: 751.2856; found 751.2860 (M+H)⁺.

Computational Details. Density functional theory (DFT) calculations^[71] were carried out using the B.01 revision of the Gaussian 16 program package,^[72] in combination with the M06-2X hybrid meta exchange–correlation functional,^[73] which has been specifically designed to work well with charge transfer excitations having intermediate spatial overlap.^[74] The Pople 6-31+G(d) basis set was used for all atoms.^[75,76] The polarizable continuum model (PCM) was employed to take in to account solvation effects (*i.e.*, toluene and dimethylformamide).^[77-79] TD-DFT calculations,^[80-82] at the same level of theory used for ground-state optimizations, were used to compute Franck-Condon excitations and to fully optimize the lowest-energy excited state (S₁) of the dyads. Natural transition orbitals (NTOs) were used to get a compact orbital representation for the computed excitations, both at the Franck-Condon regions and for relaxed excited states.^[57] The Ciofini's charge-transfer diagnostic was adopted to get a deeper insight on the photophysics of these donor-acceptor dyads.^[61,62] All the molecules were investigated within the C₂-symmetry point group. Analytical frequency calculations were always carried out to confirm the nature of the stationary points found on the potential energy surfaces of both S₀ and S₁. All the pictures of molecular orbitals and density surfaces were created using GaussView 6.^[83]

Spectroscopic Measurements. Spectrophotometric-grade toluene and dimethylformamide were used as solvent without further purification. Absorption spectra were recorded with a PerkinElmer Lambda 950 spectrophotometer. For the photoluminescence experiments, the sample solutions were placed in fluorimetric Suprasil quartz cuvettes (10.00-mm path length) at concentrations in the range 1–10 μM. The uncorrected emission spectra were obtained with an Edinburgh Instruments FLS920 spectrometer equipped with a Peltier-cooled Hamamatsu R928 photomultiplier tube (PMT) (spectral window: 185–850 nm). An Osram XBO Xenon arc lamp (450 W) was used as the excitation light source. The corrected spectra were obtained via a calibration curve, determined using an Ocean Optics deuterium-halogen calibrated lamp (DH-3plus-CAL-EXT). The photoluminescence quantum yields (PLQY) in solution were obtained from the corrected spectra on a wavelength scale (nm) and measured according to the approach described by Demas and Crosby,^[84] using an air-equilibrated water solution of quinine sulfate in 1 N H₂SO₄ as reference (PLQY = 0.546).^[85] The emission lifetimes (τ) were measured through the time-correlated single photon counting (TCSPC) technique using an HORIBA Jobin Yvon IBH FluoroHub controlling a spectrometer equipped with a pulsed NanoLED (λ_{exc} = 331 nm; 200 ps time resolution after reconvolution) as the excitation source and a red-sensitive Hamamatsu R-3237-01 PMT as the detector (spectral window: 185–850 nm). The analysis of the luminescence decay profiles was accomplished with the DAS6 Decay Analysis Software provided by the manufacturer, and the quality of the fit was assessed with the χ² value close to 1 and with the residuals regularly distributed along the time axis. To record the 77 K luminescence spectra, samples were put in quartz tubes (2 mm inner diameter) and inserted into a special quartz Dewar flask filled with liquid nitrogen. Experimental uncertainties are estimated to be ≈ 8% for lifetime determinations, ≈ 20% for PLQYs, ± 2 and ± 5 nm for absorption and emission peaks.

FULL PAPER

Acknowledgements

The financial support by CNR (PHEEL) is gratefully acknowledged.

Keywords: carbazole • donor-acceptor dyads • fluorescence • π -conjugated systems • terpyridine

- [1] L. Beverina, G. A. Pagani, *Acc. Chem. Res.* **2014**, *47*, 319-329.
- [2] H. Bohra, M. Wang, *J. Mater. Chem. A* **2017**, *5*, 11550-11571.
- [3] J. Mei, N. L. C. Leung, R. T. K. Kwok, J. W. Y. Lam, B. Z. Tang, *Chem. Rev.* **2015**, *115*, 11718-11940.
- [4] Z. Yang, Z. Mao, Z. Xie, Y. Zhang, S. Liu, J. Zhao, J. Xu, Z. Chi, M. P. Aldred, *Chem. Soc. Rev.* **2017**, *46*, 915-1016.
- [5] Z. Liu, G. Zhang, D. Zhang, *Chem.-Eur. J.* **2016**, *22*, 462-471.
- [6] J. Borges-González, C. J. Kousseff, C. B. Nielsen, *J. Mater. Chem. C* **2019**, *7*, 1111-1130.
- [7] D. Kong, Z. Xiao, Y. Gao, X. Zhang, R. Guo, X. Huang, X. Li, L. Zhi, *Mater. Sci. Eng. R Rep.* **2019**, *137*, 1-37.
- [8] K. Brunner, A. van Dijken, H. Börner, J. J. A. M. Bastiaansen, N. M. M. Kiggen, B. M. W. Langeveld, *J. Am. Chem. Soc.* **2004**, *126*, 6035-6042.
- [9] B. Souharce, C. J. Kudla, M. Forster, J. Steiger, R. Anselmann, H. Thiem, U. Scherf, *Macromol. Rapid Commun.* **2009**, *30*, 1258-1262.
- [10] Z.-S. Wang, N. Koumura, Y. Cui, M. Takahashi, H. Sekiguchi, A. Mori, T. Kubo, A. Furube, K. Hara, *Chem. Mater.* **2008**, *20*, 3993-4003.
- [11] C. B. Nielsen, S. Holliday, H.-Y. Chen, S. J. Cryer, I. McCulloch, *Acc. Chem. Res.* **2015**, *48*, 2803-2812.
- [12] N. Manfredi, B. Ceconi, A. Abbotto, *Eur. J. Org. Chem.* **2014**, *2014*, 7069-7086.
- [13] M. Magliulo, K. Manoli, E. Macchia, G. Palazzo, L. Torsi, *Adv. Mater.* **2015**, *27*, 7528-7551.
- [14] C. Zhang, P. Chen, W. Hu, *Chem. Soc. Rev.* **2015**, *44*, 2087-2107.
- [15] Z. Yang, A. Sharma, J. Qi, X. Peng, D. Y. Lee, R. Hu, D. Lin, J. Qu, J. S. Kim, *Chem. Soc. Rev.* **2016**, *45*, 4651-4667.
- [16] Y. Ha, H.-K. Choi, *Chem.-Biol. Interact.* **2016**, *248*, 36-51.
- [17] F. Bures, *RSC Adv.* **2014**, *4*, 58826-58851.
- [18] S. V. Fedoseev, M. Y. Belikov, M. Y. Ievlev, O. V. Ershov, V. A. Tafeenko, *Dyes Pigm.* **2019**, *165*, 451-457.
- [19] E. Horak, M. Robić, A. Šimanović, V. Mandić, R. Vianello, M. Hranjec, I. M. Steinberg, *Dyes Pigm.* **2019**, *162*, 688-696.
- [20] M. Kivala, F. Diederich, *Acc. Chem. Res.* **2009**, *42*, 235-248.
- [21] R. Li, Z.-L. Gong, J.-H. Tang, M.-J. Sun, J.-Y. Shao, Y.-W. Zhong, J. Yao, *Sci. China Chem.* **2018**, *61*, 545-556.
- [22] E. Ortega, J. C. Bernède, A. M. R. Ramírez, G. Louarn, F. R. Díaz, L. Cattin, M. A. del Valle, *J. Mol. Model.* **2019**, *25*, 81.
- [23] J. Tydlitát, S. Achelle, J. Rodríguez-López, O. Pytela, T. Mikýšek, N. Cabon, F. Robin-le Guen, D. Miklík, Z. Růžicková, F. Bureš, *Dyes Pigm.* **2017**, *146*, 467-478.
- [24] Z. R. Grabowski, K. Rotkiewicz, W. Rettig, *Chem. Rev.* **2003**, *103*, 3899-4032.
- [25] S. M. Bonesi, R. Erra-Balsells, *J. Lumin.* **2001**, *93*, 51-74.
- [26] A. R. Katritzky, G. W. Rewcastle, L. M. Vazquez de Miguel, *J. Org. Chem.* **1988**, *53*, 794-799.
- [27] S. E. Creutz, K. J. Lotito, G. C. Fu, J. C. Peters, *Science* **2012**, *338*, 647-651.
- [28] S. Ameen, S. B. Lee, S. C. Yoon, J. Lee, C. Lee, *Dyes Pigm.* **2016**, *124*, 35-44.
- [29] T. Zhou, B. Li, B. Wang, *Chem. Commun.* **2017**, *53*, 6343-6346.
- [30] J. Li, A. C. Grimsdale, *Chem. Soc. Rev.* **2010**, *39*, 2399-2410.
- [31] N. Blouin, M. Leclerc, *Acc. Chem. Res.* **2008**, *41*, 1110-1119.
- [32] A. K. Pal, G. S. Hanan, *Chem. Soc. Rev.* **2014**, *43*, 6184-6197.
- [33] A. Arrigo, A. Santoro, F. Puntoriero, P. P. Lainé, S. Campagna, *Coord. Chem. Rev.* **2015**, *304*, 109-116.
- [34] L. Flamigni, J.-P. Collin, J.-P. Sauvage, *Acc. Chem. Res.* **2008**, *41*, 857-871.
- [35] S. Encinas, L. Flamigni, F. Barigelletti, E. C. Constable, C. E. Housecroft, E. R. Schofield, E. Figgemeier, D. Fenske, M. Neuburger, J. G. Vos, M. Zehnder, *Chem.-Eur. J.* **2002**, *8*, 137-150.
- [36] D. J. Cardenas, J. P. Collin, P. Gavina, J. P. Sauvage, A. De Cian, J. Fischer, N. Armaroli, L. Flamigni, V. Vicinelli, V. Balzani, *J. Am. Chem. Soc.* **1999**, *121*, 5481-5488.
- [37] J. Palion-Gazda, B. Machura, T. Klemens, A. Szlapa-Kula, S. Krompiec, M. Siwy, H. Janeczek, E. Schab-Balcerzak, J. Grzelak, S. Maćkowski, *Dyes Pigm.* **2019**, *166*, 283-300.
- [38] M. Toshiki, A. Koji, *Curr. Org. Chem.* **2007**, *11*, 195-211.
- [39] W. Goodall, K. Wild, K. J. Arm, J. A. G. Williams, *J. Chem. Soc., Perkin Trans. 2* **2002**, 1669-1681.
- [40] A. Winter, A. M. J. van den Berg, R. Hoogenboom, G. Kickelbick, U. S. Schubert, *Synthesis* **2006**, 2873-2878.
- [41] J. Wang, G. S. Hanan, *Synlett* **2005**, 1251-1254.
- [42] G. Accorsi, N. Armaroli, F. Cardinali, D. Wang, Y. Zheng, *J. Alloys Compd.* **2009**, *485*, 119-123.
- [43] X. Chen, Q. Zhou, Y. Cheng, Y. Geng, D. Ma, Z. Xie, L. Wang, *J. Lumin.* **2007**, *126*, 81-90.
- [44] T. He, Y. Gao, R. Chen, L. Ma, D. Rajwar, Y. Wang, A. C. Grimsdale, H. Sun, *Macromolecules* **2014**, *47*, 1316-1324.
- [45] S.-H. Hwang, P. Wang, C. N. Moorefield, L. A. Godinez, J. Manriquez, E. Bustos, G. R. Newkome, *Chem. Commun.* **2005**, 4672-4674.
- [46] C. Kong, M. Peng, H. Shen, Y. Wang, Q. Zhang, H. Wang, J. Zhang, H. Zhou, J. Yang, J. Wu, Y. Tian, *Dyes Pigm.* **2015**, *120*, 328-334.
- [47] Q. Liu, X. Yang, M. Wang, D. Liu, M. Chen, T. Wu, Z. Jiang, P. Wang, *Tetrahedron* **2019**, *75*, 2400-2405.
- [48] A. Maron, A. Szlapa, T. Klemens, S. Kula, B. Machura, S. Krompiec, J. G. Malecki, A. Switlicka-Olszewska, K. Erfurt, A. Chrobok, *Org. Biomol. Chem.* **2016**, *14*, 3793-3808.
- [49] A. Baschieri, L. Sambri, I. Gualandi, D. Tonelli, F. Monti, A. D. Esposti, N. Armaroli, *RSC Adv.* **2013**, *3*, 6507-6517.
- [50] J. H. Cho, Y. S. Ryu, S. H. Oh, J. K. Kwon, E. K. Yum, *Bull. Korean Chem. Soc.* **2011**, *32*, 2461-2464.
- [51] Y. Hirata, *Bull. Chem. Soc. Jpn.* **1999**, *72*, 1647-1664.
- [52] J. Saltiel, V. K. Kumar, *J. Phys. Chem. A* **2012**, *116*, 10548-10558.
- [53] H. Suzuki, *Bull. Chem. Soc. Jpn.* **1959**, *32*, 1340-1350.
- [54] R. Fukuda, M. Ehara, *Phys. Chem. Chem. Phys.* **2013**, *15*, 17426-17434.
- [55] K. Okuyama, T. Hasegawa, M. Ito, N. Mikami, *J. Phys. Chem.* **1984**, *88*, 1711-1716.
- [56] M. Mitsui, Y. Kawano, R. Takahashi, H. Fukui, *RSC Adv.* **2012**, *2*, 9921-9931.
- [57] R. L. Martin, *J. Chem. Phys.* **2003**, *118*, 4775-4777.
- [58] T. Yanai, D. P. Tew, N. C. Handy, *Chem. Phys. Lett.* **2004**, *393*, 51-57.
- [59] J. D. Chai, M. Head-Gordon, *Phys. Chem. Chem. Phys.* **2008**, *10*, 6615-6620.
- [60] A. Dreuw, M. Head-Gordon, *J. Am. Chem. Soc.* **2004**, *126*, 4007-4016.
- [61] T. Le Bahers, C. Adamo, I. Ciofini, *J. Chem. Theory Comput.* **2011**, *7*, 2498-2506.
- [62] C. Adamo, T. Le Bahers, M. Savarese, L. Wilbraham, G. García, R. Fukuda, M. Ehara, N. Rega, I. Ciofini, *Coord. Chem. Rev.* **2015**, *304*-305, 166-178.
- [63] R. Improta, V. Barone, G. Scalmani, M. J. Frisch, *J. Chem. Phys.* **2006**, *125*, 054103.
- [64] R. Improta, G. Scalmani, M. J. Frisch, V. Barone, *J. Chem. Phys.* **2007**, *127*, 074504.
- [65] M. Z. Zgierski, E. C. Lim, *Chem. Phys. Lett.* **2004**, *387*, 352-355.
- [66] M. Z. Zgierski, T. Fujiwara, E. C. Lim, *Acc. Chem. Res.* **2010**, *43*, 506-517.
- [67] K. Y. Chai, D. H. Lee, H. M. Hwang, Korea, **2014**.
- [68] A. Z. Muresan, P. Thamyongkit, J. R. Diers, D. Holten, J. S. Lindsey, D. F. Bocian, *The Journal of Organic Chemistry* **2008**, *73*, 6947-6959.

FULL PAPER

- [69] L. Rigamonti, B. Babgi, M. P. Cifuentes, R. L. Roberts, S. Petrie, R. Stranger, S. Righetto, A. Teshome, I. Asselberghs, K. Clays, M. G. Humphrey, *Inorg. Chem.* **2009**, *48*, 3562-3572.
- [70] R. Flamini, I. Tomasi, A. Marrocchi, B. Carlotti, A. Spalletti, *J. Photochem. Photobiol. A* **2011**, *223*, 140-148.
- [71] R. G. Parr, W. Yang, *Density Functional Theory of Atoms and Molecules*, Oxford University Press, Oxford, U.K., **1989**.
- [72] M. J. Frisch, G. W. Trucks, H. B. Schlegel, G. E. Scuseria, M. A. Robb, J. R. Cheeseman, G. Scalmani, V. Barone, G. A. Petersson, H. Nakatsuji, X. Li, M. Caricato, A. V. Marenich, J. Bloino, B. G. Janesko, R. Gomperts, B. Mennucci, H. P. Hratchian, J. V. Ortiz, A. F. Izmaylov, J. L. Sonnenberg, Williams, F. Ding, F. Lipparini, F. Egidi, J. Goings, B. Peng, A. Petrone, T. Henderson, D. Ranasinghe, V. G. Zakrzewski, J. Gao, N. Rega, G. Zheng, W. Liang, M. Hada, M. Ehara, K. Toyota, R. Fukuda, J. Hasegawa, M. Ishida, T. Nakajima, Y. Honda, O. Kitao, H. Nakai, T. Vreven, K. Throssell, J. A. Montgomery Jr., J. E. Peralta, F. Ogliaro, M. J. Bearpark, J. J. Heyd, E. N. Brothers, K. N. Kudin, V. N. Staroverov, T. A. Keith, R. Kobayashi, J. Normand, K. Raghavachari, A. P. Rendell, J. C. Burant, S. S. Iyengar, J. Tomasi, M. Cossi, J. M. Millam, M. Klene, C. Adamo, R. Cammi, J. W. Ochterski, R. L. Martin, K. Morokuma, O. Farkas, J. B. Foresman, D. J. Fox, Gaussian Inc., Wallingford, CT, USA, **2016**.
- [73] Y. Zhao, D. G. Truhlar, *Theor. Chem. Acc.* **2008**, *120*, 215-241.
- [74] R. Li, J. Zheng, D. G. Truhlar, *Phys. Chem. Chem. Phys.* **2010**, *12*, 12697-12701.
- [75] G. A. Petersson, A. Bennett, T. G. Tensfeldt, M. A. Al - Laham, W. A. Shirley, J. Mantzaris, *J. Chem. Phys.* **1988**, *89*, 2193-2218.
- [76] G. A. Petersson, M. A. Al - Laham, *J. Chem. Phys.* **1991**, *94*, 6081-6090.
- [77] J. Tomasi, M. Persico, *Chem. Rev.* **1994**, *94*, 2027-2094.
- [78] J. Tomasi, B. Mennucci, R. Cammi, *Chem. Rev.* **2005**, *105*, 2999-3093.
- [79] C. J. Cramer, D. G. Truhlar, Continuum Solvation Models, in *Solvent Effects and Chemical Reactivity* Vol. 17 (Eds.: O. Tapia, J. Bertrán), Springer Netherlands, **2002**, pp. 1-80.
- [80] R. E. Stratmann, G. E. Scuseria, M. J. Frisch, *J. Chem. Phys.* **1998**, *109*, 8218-8224.
- [81] M. E. Casida, C. Jamorski, K. C. Casida, D. R. Salahub, *J. Chem. Phys.* **1998**, *108*, 4439-4449.
- [82] R. Bauernschmitt, R. Ahlrichs, *Chem. Phys. Lett.* **1996**, *256*, 454-464.
- [83] R. Dennington, T. A. Keith, J. M. Millam, Semichem Inc., Shawnee Mission, KS, USA, **2016**.
- [84] G. A. Crosby, J. N. Demas, *J. Phys. Chem.* **1971**, *75*, 991-1024.
- [85] S. R. Meech, D. Phillips, *J. Photochem.* **1983**, *23*, 193-217.

FULL PAPER

Table of Contents

Layout 1

FULL PAPER

D- π -A systems. Seven Carbazole-Terpyridine π -bridged donor-acceptor systems have been synthesized and characterized. With the help of DFT calculations, the correlation between the specific structure of the bridge and the photophysical properties of the whole system has been fully elucidated.



Elia Matteucci, Andrea Baschieri,* Letizia Sambri,* Filippo Monti,* Eleonora Pavoni, Elisa Bandini, Nicola Armaroli

Page No. – Page No.

Carbazole-terpyridine donor-acceptor systems with rigid π -conjugated bridges